ELSEVIER

Physica E 10 (2001) 411–418

PHYSICA E

www.elsevier.nl/locate/physe

Neutron diffraction and reflectivity studies of interlayer correlations in magnetic semiconductor superlattices

T.M. Giebultowicz[a,*], H. Kepa[b], J. Blinowski[b], P. Kacman[c]

[a] *Department of Physics, Oregon State University, 301 Weniger Hall, Corvallis, OR 97331-6507, USA*
[b] *Department of Physics, Warsaw University, ul. Hoza 69, 00-681 Warsaw, Poland*
[c] *Inst. of Physics, Polish Acad. of Scien., Al. Lotnikow 32/46, 02-668 Warsaw, Poland*

Abstract

An overview of neutron scattering studies on two classes of magnetic semiconductor superlattices, MnTe/II-Te (II=Cd, Zn) and Eu-VI/Pb-VI (VI=S, Te) is presented. Diffraction experiments reveal distinct correlations between layers of MnTe even though they are antiferromagnetic (AFM) and the systems are nearly-insulating. Current theory status is discussed. In EuTe/PbTe, pronounced correlations between AFM EuTe blocks are also seen. In EuS/PbS, the only ferromagnetic (FM) system in the group, neutron diffractometry and reflectometry show strong AFM correlations between the FM EuS block. A tight-binding model is used in both Eu-based systems to explain interaction transfer across the non-magnetic block without the assistance of carriers.

PACS: 75.50 Pp; 75.50.Ee; 75.70

Keywords: Semiconductors; Ferromagnets; Superlattices; Correlations

1. Introduction

One highly interesting effect recently observed in heterostructures made of the newest-generation III–V-based ferromagnetic (FM) semiconductors [1,2] is magnetic coupling between two Ga(Mn)As films separated by up to 30 Å of pure non-magnetic GaAs. The fact that in Ga(Mn)As the carrier concentration attains values close to those in typical metals suggests that in the Ga(Mn)As/GaAs/Ga(Mn)As trilayers the coupling is also conveyed by a carrier-assisted mechanism similar to those responsible for coupling between FM films in metallic superlattices (SLs) (see e.g., [3]). It should be noted however, that magnetic coupling across spacers thicker than 30 Å was observed in other all-semiconductor structures grown made of materials in which the density of carriers is several orders of

* Corresponding author. Tel.: +1-541-737-1707; fax: +1-541-737-1683.
E-mail address: tgiebult@physics.orst.edu (T.M. Giebultowicz).

1386-9477/01/$ - see front matter
PII: S1386-9477(01)00128-X

magnitude lower than in metals [4–10]. Although not all results from those systems are yet clearly understood, the experimental facts provide strong evidence that there exist specific mechanisms in semiconductors capable of transferring magnetic interactions across thick non-magnetic layers without the assistance of mobile carriers.

In this paper, we present an overview of the results of interlayer coupling studies in two families of all-semiconductor magnetic SLs. Experimental search for such effects was started in the early 1990s. At that time the systems available for experimentation were made exclusively from antiferromagnetic (AFM) compounds (EuTe, MnTe). The only research tool capable of detecting correlations between AFM layers is neutron diffraction. Hence, this method played a key role in the studies on interlayer correlations. Recently, a successful technology of fabricating EuS/PbS SLs has been developed [11]. It made possible the use of neutrons for investigating correlations between FM semiconducting layers. One can, in principle, detect such correlations by other methods (e.g., SQUID magnetometry). Yet, neutron tools – conventional diffractometry and the technique of *neutron reflectometry* which is particularly well suited for studying thin FM layers – still play a leading role in this research, as they offer a more direct insight into the correlation than other experimental methods.

2. Neutron scattering tools

The following symbol will used below for describing SL structures: m and n – the number of monolayers, respectively, in a single magnetic and nonmagnetic layer; d – spacing between monolayers, and $D = (m + n)d$ – the SL period.

There are two powerful neutron scattering techniques that can be used for studying magnetic superlattices: conventional ("wide-angle") diffraction, see e.g., [12] and neutron reflectometry, see e.g., [13]. In *diffraction regime*, neutrons directly probe the correlations between individual magnetic atoms. Therefore, this method can be used for studying both FM and AFM spin structures. Also, diffraction "sees" correlations between larger groups of ordered spins (e.g., magnetic layers in a SL structure). An important function in the theory of diffraction from superlattices is the magnetic structure factor for a single SL cell (or, equivalently, a single layer):

$$F_{\text{s.l.}}(Q_z) = \sum_{k=1}^{m} M_k e^{ikdQ_z} \tag{1}$$

where Q_z is the *Q-vector* component along the SL growth axis, and M_k is the net magnetization of the kth monolayer. The $|F_{\text{s.l.}}(Q_z)|^2$ function has the shape of a broad (FWHM $\cong 2\pi/md$) maximum accompanied by weak subsidiary maxima (Fig. 1a). It describes the line shape one would obtain in a Q_z scan through a magnetic Bragg points in diffraction from a *single layer*.

If there are no magnetic correlations between successive layers, there is no coherence in scattering and the line shape from such a sample essentially reproduces the shape of $|F_{\text{s.l.}}(Q_z)|^2$. If the layers are correlated, the spectrum consist of sharp diffraction lines with even spacing $\Delta Q_z = 2\pi/D$ apart. These peaks are 'enveloped' by the $|F_{\text{s.l.}}(Q_z)|^2$ function, which produces characteristic groups of peaks ('satellites') in the Bragg point regions. As shown in panels (b) and (c) in Fig. 1, there is a distinct difference between the peak patterns for FM and AFM correlations between layers. For FM correlations there is a central line at the Bragg point, whereas AFM ones produce an intensity *minimum* at the same spot.

Neutron reflectometry. When scattered at very small angles from a flat specimen, the neutrons no longer "see" individual atomic momenta but the net magnetization within the material. If ferromagnetic layers in a SL structure are all magnetized in the same direction (FM correlations), than the magnetic periodicity D_{FM} is the same as the "chemical" one (D), and magnetic Bragg peaks occur at the same positions as the structural peaks (Fig. 2a). For alternating magnetization (AFM interlayer correlations) the magnetic periodicity is $D_{\text{AFM}} = 2D$, and the peaks occur half-way in between the structural ones (Fig. 2b). It should be noted that the intensity and resolution in reflectometry is considerably better than in diffraction experiments. However, this method cannot be used for studying AFM layers in which $\boldsymbol{B}$ is always zero due to the zero net moment.

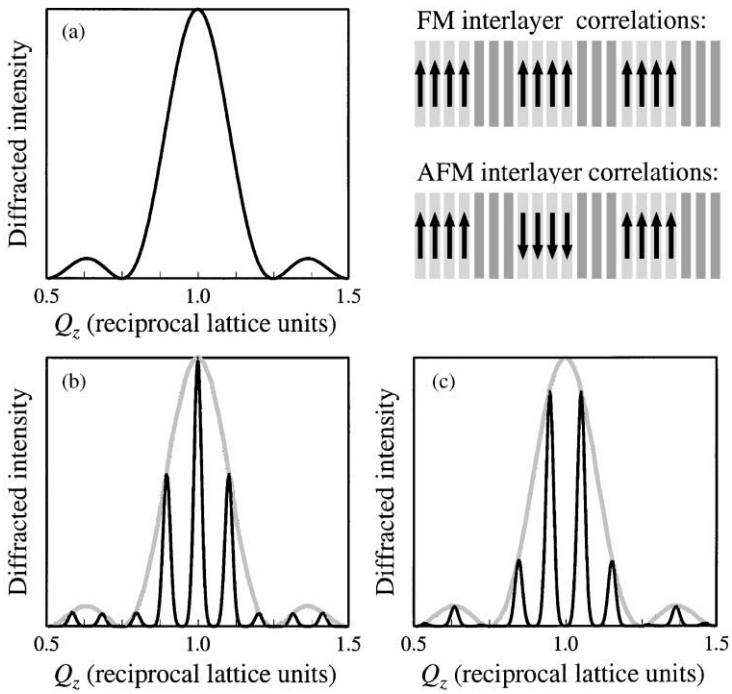

Fig. 1. Diffraction profiles for: (a) uncorrelated superlattice (the profile reproduces the shape of the squared single-layer structure factor $|F_{\mathrm{s.l.}}|^2$); (b) a superlattice with FM correlations between FM layers; (c) a one with AFM correlations between FM layers.

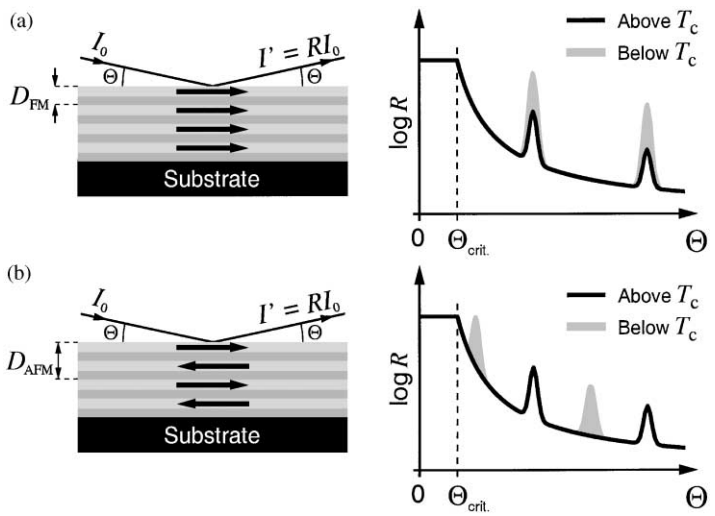

Fig. 2. Reflectivity profiles from a multilayered structure with: (a) FM, and (b) AFM correlations between ferromagnetic layers. The maxima in the solid curve are the structural Bragg peaks, and the shaded profiles show the positions of the magnetic peaks arising below T_c.

3. Overview of experimental and model results

3.1. II–VI based systems

II–VI/Mn-VI superlattices were the first magnetic semiconductor epitaxial structures investigated by neutron techniques [7,14,15]. In these epitaxial systems the magnetic constituents, MnSe and MnTe, crystallize in the metastable zinc blende (ZB) structure that does not form in bulk. These ZB modifications are strongly frustrated FCC antiferromagnets that at low temperatures form the so-called Type III AFM structure, an arrangement with a tetragonal magnetic unit cell a, a, $2a$ (where a is the lattice constant of the chemical FCC cell).

Pronounced interlayer coupling effects were observed in two II–VI/Mn-VI structures, CdTe/MnTe and ZnTe/MnTe with [0 0 1] growth axis [4–6]. Although the chemical formulae are very similar, these two systems are magnetically quite different. This comes from the fact that the Type III AFM order in the frustrated spin lattices is very sensitive to symmetry-breaking strains.

The unstrained cubic lattice parameters for CdTe and ZB MnTe are $a_{\mathrm{CdTe}} = 6.48$ Å and $a_{\mathrm{MnTe}} = 6.34$ Å. Because of such mismatch, in the CdTe/MnTe structures the MnTe layers are *stretched* – the lattice period a_{xy} along the [1 0 0] and [0 1 0] in-plane axes is elongated, while the period (a_z) in the [0 0 1] growth direction is shortened ($a_z < a_{\mathrm{MnTe}} < a_{xy}$). Such a lattice distortion causes a transition from the commensurate Type III order to a new structure in which the Mn spin directions are arranged in a helical fashion [14]. The axis of the spin helix is parallel to one of the in-plane axes, and the helix pitch is *incommensurate* with the atomic lattice period. In other words, the spin lattice periodicity along the principal crystallographic axes is now $(2+\delta)a_{xy}$, a_{xy}, a_z.

Neutron diffraction studies of the CdTe/MnTe system [6] were performed on a number of ALE-grown samples in which the MnTe layer thickness was kept approximately constant (ca. 10 mls.), and the CdTe spacer thickness was changed from 2 to 14 mls. As expected, the pitch $2+\delta$ of the helical order seen in the samples gradually increased with increasing spacer thickness. In addition, in samples with CdTe spacer thickness up to 30 Å, Q-scans performed in the z direction revealed distinct patterns of interference fringes, showing that the spin helices forming in successive layers are phase-synchronized. Such an effect clearly indicates the existence of some kind of 'magnetic communication' between the MnTe layers across the non-magnetic CdTe blocks. This interaction certainly cannot be mediated by carriers, as in the case of metallic SLs, because both MnTe and CdTe are nearly perfect insulators at low temperatures.

A theoretical explanation of the effects seen in the CdTe/MnTe has been recently proposed by Rusin [16] who pointed out that even though there are no *mobile* carriers in the system at low T, CdTe does contain carriers that are bound by impurities or defects, forming 'hydrogenic centers' with the Bohr radius of several tens of Å. In diluted magnetic semiconductors such centers may polarize magnetic ions within the Bohr orbit, giving rise to an effect known as 'bound magnetic polaron' (BMP). In short, in the Rusin's model the centers located in the spacer act in a similar way on the interface Mn spins from the two adjacent MnTe blocks, 'synchronizing' their polarization and thus effectively introducing magnetic coupling between the spin helices.

In contrast to CdTe/MnTe, in ZnTe/MnTe the MnTe layers are *compressed* because $a_{\mathrm{ZnTe}} = 6.10$ Å. Such a distortion of the FCC lattice does not change the Type III AFM order but only selects an energy-minimizing configuration with the unit cell doubling direction along the SL growth axis (i.e., the magnetic cell parameters are a_{xy}, a_{xy}, $2a_z$) [15]. Neutron diffraction data from specimens with thin non-magnetic ZnTe spacers reveal pronounced interlayer coupling effects. The interference fringes were observed for ZnTe thickness up to 15 Å [5,6], so the coupling range is somewhat shorter than in CdTe/MnTe. However, the coupling shows an unusual temperature behavior, not seen in that latter system. Diffraction data from a $[(\mathrm{ZnTe})_5|(\mathrm{MnTe})_{10}]_{400}$ sample are displayed in Fig. 3. The spectrum measured at 10 K shows a central peak accompanied by two maxima at the calculated first-order satellite positions S_{-1} and S_{+1} – but one can also see weak peaks emerging at 'half-integer' satellite positions $S_{-1/2}$ and $S_{+1/2}$. When the temperature is raised, the central peak gradually disappears while the $S_{-1/2}$, $S_{+1/2}$ peaks increase and become the dominant spectrum features. Such a behavior clearly indicates that with the increase of T the *sign* of the interlayer interaction

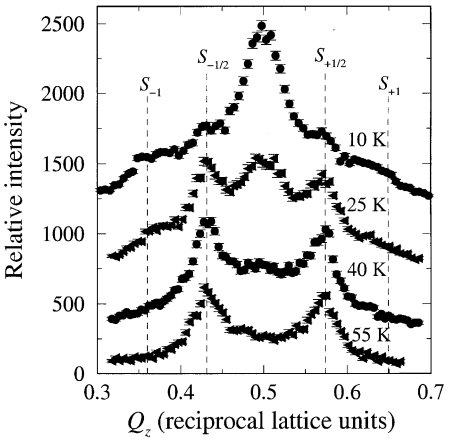

Fig. 3. Magnetic diffraction spectra from a $[(ZnTe)_{10}|(MnTe)_5]_400$ specimen measured at different temperatures. The low-T data show a central peak and weak satellites as S_{-1} and S_{+1} positions and additional weak satellites at $S_{-1/2}$ and $S_{+1/2}$ positions. With increasing T, the central peak gradually disappears, whereas the $S_{-1/2}$ and $S_{+1/2}$ peaks increase in intensity, indicating a change form 'positive' correlations to 'anticorrelations' (after [17]).

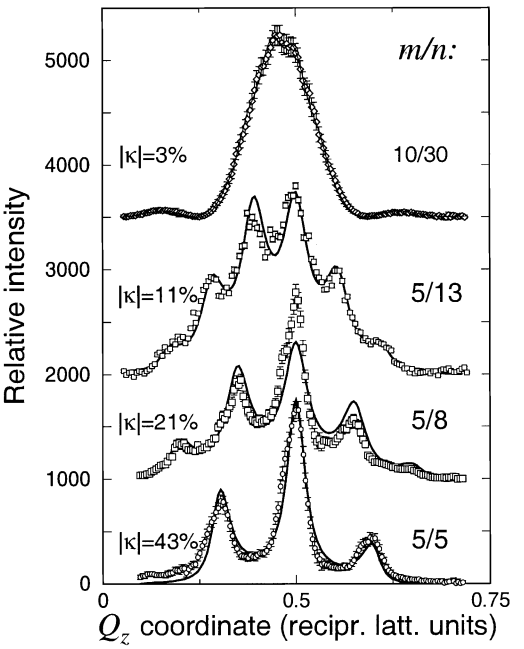

Fig. 4. Measured magnetic diffraction peak profiles from several $[(EuTe)_m|(MnTe)_n]_N$ superlattice samples, illustrating a gradual transition from strong interlayer coupling for smaller n values to an almost completely uncorrelated state in a system with $n = 30$. The solid curves are fits of Eq. (4) to the data points. The fitted values of the 'partial correlation coefficient' $|\kappa|$ for each spectrum is shown in the figure (after [19]).

changes. The mechanism responsible for this peculiar behavior is not yet clearly understood. An interesting new development in the ZnTe/MnTe studies are the latest data from samples doped with Cl, which introduces deep electronic levels in ZnTe [6]. The doping was found to enhance the low-T correlations, but not to significantly influence the system behavior for $T > 40$ K, still providing no clue as to the reason why the interaction sign changes.

3.2. EuTe and EuS based systems

EuTe/PbTe is another AFM semiconductor superlattice system that has been thoroughly studied by neutron diffractometry. $[(EuTe)_m|(PbTe)_n]_N$ samples with [1 1 1] growth axis prepared by MBE on BaF_2 substrates are of remarkably good crystalline quality [18]. EuTe is an FCC antiferromagnet with $T_N = 9.6$ K. However, its spin structure (known as the Type II AFM ordering) is quite different from that seen in MnTe. The Eu spins are arranged into ferromagnetic 'sheets' on (1 1 1)-type planes, and these sheets are antiferromagnetically coupled to one another.

Neutron diffraction studies [7,8,18], carried out on a large population ($\sim$ 50) of specimens with many different combinations of m and n, have revealed distinct interlayer correlation satellites in samples with n up to 20. It shows that the interaction between adjacent EuTe can be transferred across non-magnetic PbTe spacers as thick as 70 Å (note this over 2 times more than the longest transfer range observed in the MnTe-based systems).

However, as can be seen in Fig. 4, with increasing n the satellite peaks become less sharp, while a pronounced 'hump' appears underneath; the initial set of well-resolved lines gradually changes into the characteristic smooth profile of the $|F_{s.l.}(Q_z)|^2$ function. This process indicates that the interlayer correlations gradually weaken with the increasing PbTe thickness. In order to describe this process in a quantitative way, a model has been developed in which it is assumed that the spin structure in individual EuTe layer is not completely uniform – rather, each layer consists of a large number of domains (actually, there is much

evidence supporting such a scenario). Two domains facing one another across a PbTe spacer may be either positively correlated or anticorrelated. Let $\mathscr{P}$ be the fraction positively correlated domain pairs in two successive layers. For $\mathscr{P}=1$ neutrons would see the system as perfectly positively correlated, for $\mathscr{P}=\frac{1}{2}$ – as perfectly random, and for $\mathscr{P}=-1$ – as perfectly anticorrelated. The *fractional correlation coefficient* defined as $\kappa=2\mathscr{P}-1$ in these three cases takes, respectively, the values: $+1, 0$, and -1, whereas a fractional κ value means partial correlations. It can be shown that for $|\kappa|<1$ the neutron diffraction spectrum shape is described by an analytical expression [20]:

$$I(Q_z) \propto \frac{f^2(Q_z)|F_{\text{s.l.}}(Q_z)|^2(1-\kappa^2)}{1-2\kappa\cos(Q_z D)+\kappa^2}. \tag{2}$$

Fits to the measured data plotted in Fig. 4 show that this simple function describes the observed spectrum profiles remarkably well.

Because the carrier concentration in the EuTe/PbTe system is several orders of magnitude lower than in metals (10^{16}–10^{17} cm^{-3}), the observed coupling cannot be attributed to RKKY interaction or any other carrier-assisted mechanism. What additionally argues against an interpretation involving carriers is the fact that elevating the electron concentration in the spacers to $\sim 10^{19}$ cm^{-3} (by doping with Bi) does not enhance the correlations [19]. It should also be noted that the coupling model proposed by Rusin [16] for the CdTe/MnTe system cannot be applied to EuTe/PbTe because there are no donor centers of the right type in PbTe. In search for a physical mechanism that could explain the pronounced coupling effects seen in the experiments, two of us (JB and PK) [21] explored the possibility that the interlayer interactions are conveyed by the valence electronic states. The sensitivity of the total energy of the valence electrons was investigated using a simple 1-D tight-binding model. The band structure was calculated for two different spin configurations in successive EuTe layers: perfect correlations ($\cdots\uparrow\downarrow\uparrow\downarrow\cdots\uparrow\downarrow\uparrow\downarrow\cdots$) and perfect 'anticorrelations' ($\cdots\uparrow\downarrow\uparrow\downarrow\cdots\downarrow\uparrow\downarrow\uparrow\cdots$). The respective energies, E' and E'', indeed appear to be different. Thus, states with correlated alignment of spins in successive layers lead to lower total energy than states with a random succession of alignments. $\Delta E=E'-E''$ has the physical meaning of interlayer coupling energy. The results of calculations show that ΔE is a rather slowly decreasing function of the spacer thickness n, which is consistent with long range of the observed coupling. A quantitative comparison of the model and experimental data is not easy because the energy of coupling between the AFM EuTe blocks cannot be directly measured by neutron diffraction. However, it seems to be a reasonable assumption that the value of the 'fractional correlation coefficient' κ reflects the interlayer coupling strength. As shown in Fig. 5, a plot of the fitted $|\kappa|$ values vs. n for a series of samples with $m=5$ is remarkably similar to the calculated $\Delta E(n)$ characteristic, which certainly provides a strong support for the model.

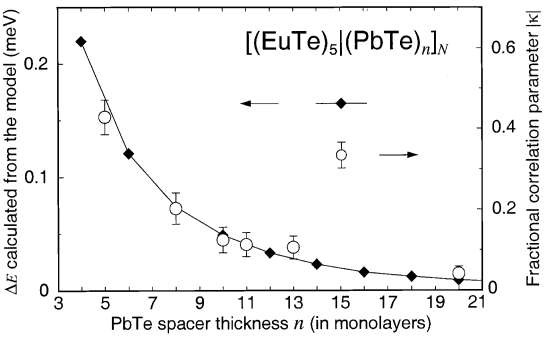

Fig. 5. Calculated interlayer coupling energy ΔE vs. n characteristic for EuTe/PbTe superlattices with $m=5$, the fitted $|\kappa|$ values obtained for several samples with $m=5$ and different n values, plotted in one field. The graph shows that ΔE and $|\kappa|$ change with n in a remarkably similar way. Note the vertical scales for ΔE and $|\kappa|$ are different (after [19]).

EuS/PbS is another SL structure based on the Eu chalcogenides that has been investigated by neutron tools [9,10]. EuS is a FCC ferromagnet with $T_c=16.6$ K. The SL specimens were prepared on KCl substrates with a [0 0 1] growth axis. Diffraction scans carried out at low temperatures revealed magnetic spectra with a characteristic double-peak profile (Fig. 6) – a clear signature of *antiferromagnetic* coupling between the FM layers. This AFM interlayer coupling showed up even more clearly in reflectivity spectra (Fig. 7) which exhibited sizable maxima at positions corresponding to the doubled structural periodicity of the measured specimen. Such peaks were observed for systems with then non-magnetic spacer thickness D_{PbS} up to 90 Å.

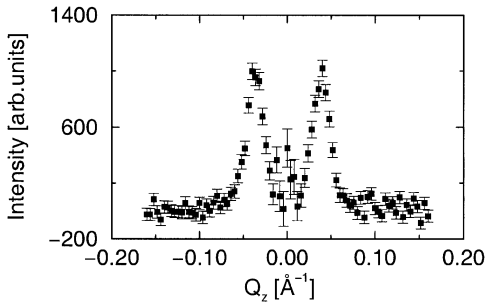

Fig. 6. Diffraction spectrum from a EuS/PbS SL specimen with a $(60,23\ \text{Å})\times 30$ composition at 4.3 K. Purely magnetic contribution obtained by subtracting data sets taken below and above T_c. The characteristic double-peaked profile is a clear signature of AFM coupling between the EuS layers (after [19]).

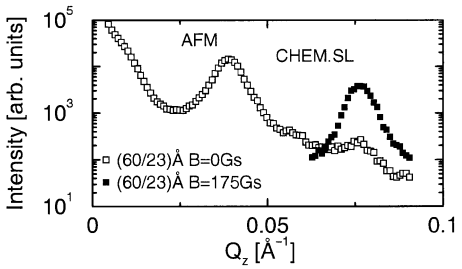

Fig. 7. Reflectivity data at 4.3 K from the same specimen used for obtaining data shown in Fig. 7. The spectrum at zero field (blank data points) exhibits a small structural peak due to chemical SL periodicity, and a large peak corresponding to doubled SL periodicity arising from AFM coupling between EuS layers. An external field of 175 G enforces a transition to a FM configuration, so the magnetic peak shifts to the structural position (filled points).

The fact that the FM layers have a net magnetic moment makes it possible to manipulate the arrangement of layers in the SL chain. A sufficiently strong external magnetic field enforces a transition to a FM sequence. For D_{PbS} up to about 20 Å, this process was found to be reversible. In this region, the field B_{sat} needed to attain a full AFM→FM transition provides a direct measure of the interlayer coupling strength. For thicker spacers the EuS layers do not return to the AFM configuration even after removing the field, evidently locked in the FM positions by magnetic anisotropy. Here the B_{sat} value reflects the anisotropy magnitude rather then the coupling strength.

Model studies on EuS/PbS were performed using the same tight-binding approach as in the earlier work on the EuTe/PbTe system [10]. Since the atomic monolayers in SLs with [0 0 1] growth axis consist of both anions and cations (in contrast to the situation in the [1 1 1] EuTe/PbTe structures which consists of alternating anion-only and cation-only monolayers), a more sophisticated 3D model version had to be constructed than the previously used 1D chain. From the calculations it was obtained that an AFM alignment of layers *always* leads to lower energy than the FM one, in accord with the experiments which showed only AFM coupling in all investigated samples. The calculated coupling strength decreases with the PbS spacer thickness roughly like 2^{-n}. Such a fast decrease is also consistent with the observations. The model also passes favorably a basic quantitative test, as the calculated coupling energy values are of the same order of magnitude as the values determined from the observed saturation fields B_{sat}.

4. Closing remarks

Neutron diffraction experiments on the MnTe/II-Te and EuTe/PbTe multilayers have demonstrated two important facts: (i) pronounced a interlayer magnetic coupling may occur in superlattices made of nearly-insulating semiconductors; (ii) in such systems, coupling between AFM layers is possible.

The results model studies discussed in Section 3 show that the transfer of interactions without the assistance of carriers may be explained on the grounds of the electronic theory of semiconductor. However, much more theoretical and experimental insight is still needed. The mechanism proposed by Rusin [16] is definitely of great interest because it offers the possibility of controlling the coupling strength. Yet, the model requires testing by additional experiments. The change of interaction sign seen in ZnTe/MnTe is indeed extremely intriguing; hopefully a theoretical explanation of this phenomenon will soon emerge. The Eu-VI/Pb-VI structures are quite attractive from the viewpoint of theoretical analysis because the same formalism is used to the AFM EuTe/PbTe and the FM EuS/PbS. Some model elements can be tested

by experiments on EuS/PbS and then used for explaining effects seen in EuTe/PbTe, for which it is not possible to directly measure the strength of interlayer coupling. For instance, the coupling energies for EuS/PbS obtained from the model show a weak dependence on the EuS layer thickness, indicating that the interface monolayers play a principle role in the coupling mechanism. If this prediction is verified by experiments, the reason why coupling between AFM EuTe layers is possible will become clearly understood.

Acknowledgements

Support of NSF and NATO Grants for work on the Eu-based system presented in this work is gratefully acknowledged.

References

[1] H. Ohno, Science 281 (1998) 951.
[2] T. Dietl, H. Ohno, F. Matsukura, J. Ciberd, D. Ferrand, Science 287 (2000) 1019.
[3] B.A. Jones, IBM J. of Res. Dev. 42 (1998) 25.
[4] V. Nunez, T.M. Giebultowicz, W. Fashinger, G. Bauer, H. Sitter, J.K. Furdyna, Material Res. Soc. Symp. Proc. 376 (1995) 589.
[5] J. Lin, J.J. Rhyne, J.K. Furdyna, T.M. Giebultowicz, J. Appl. Phys. 83 (1998) 6554.
[6] L.E. Stumpe, J.J. Rhyne, H. Kaiser, S. Lee, U. Bindley, J.K. Furdyna, J. Appl. Phys. 87 (2000) 6460.
[7] T.M. Giebultowicz et al., Physica B 198 (1994) 163.
[8] H. Kepa et al., Physica E 2 (1998) 399.
[9] H. Kepa et al., ICM2000 Proceedings, Physica B (2000), in print.
[10] H. Kepa et al., in preparation.
[11] A. Stachow-Wojcik et al., Phys. Rev. B 60 (1999) 15220.
[12] G.E. Bacon, Neutron Diffraction, Clarendon Press, Oxford, 1975.
[13] C.F. Majkrzak, Physica B 173 (1991) 75.
[14] T.M. Giebultowicz, N. Samarth, H. Luo, J.K. Furdyna, P. Klosowski, J.J. Rhyne, Phys. Rev. B 46 (1992) 12076.
[15] T.M. Giebultowicz, P. Klosowski, N. Samarth, H. Luo, J.K. Furdyna, J.J. Rhyne, Phys. Rev. B 48 (1992) 12817.
[16] T.M. Rusin, Phys. Rev. B 58 (1998) 2107.
[17] T.M. Giebultowicz, V. Nunez, H. Luo, J.K. Furdyna, J.J. Rhyne, 1994, unpublished.
[18] G. Springholz, G. Bauer, Appl. Phys. Lett. 62 (1993) 2399.
[19] H. Kepa, G. Springholz, T.M. Giebultowicz et al., in preparation.
[20] K.I. Goldman, Thesis, Oregon State University, 1998, unpublished.
[21] J. Blinowski, P. Kacman, Acta Physica Polonica A 19 (1997) 719.